Heat pipes thermal performance for a reversible thermoelectric cooler-heat pump for a nZEB

P. Aranguren[1,2*], S. DiazDeGarayo[3], A. Martínez[1,2], D. Astrain[1,2]

[1] *Mechanical, Energy and Materials Engineering Department Public University of Navarre, 31006 Pamplona, Spain*

[2] *Smart Cities Institute, Pamplona, Spain*

[3] *National Renewable Energy Centre, 31621 Sarriguren, Spain*

[*] *e-mail:patricia.arangureng@unavarra.es*

Keywords: thermoelectric cooler; thermoelectric heat pump; nZEB; Air conditioning; computational optimization

Abstract

The nZEB standards reduce the energy demand of these buildings to a minimum, obtaining this little energy from renewable resources. Taking these aspect into consideration, a thermoelectric cooler-heat pump is proposed to achieve the comfort temperature along the whole year. The same device can provide heat in winter and it can cool down the buildings in summer just by switching the voltage supply polarity. Heat pipes are studied to work on both sides of the thermoelectric modules in order to optimize the heat transfer as these devices present really good thermal resistances and they can work in any position. However, they present pretty different thermal resistances if they work on the cold or on the hot side of the modules. A methodology to thermally characterize these heat exchangers working in both orientations is proposed and a validated computational model is developed to optimize the thermoelectric cooler-heat pump for a nZEB application. The number of thermoelectric modules, the position of the device, the ambient temperature and the air mass flow determine the operation and consequently they need to be studied in order to optimize the application.

Nomenclature

α	Seebeck coefficient	V/K
ΔT	Difference in temperature from the heat source to the heat sink	ºC
ρ	Density	Kg/m^3
A	Cross sectional area	m^2
$b_{R^{TEM}}$	Systematic standard uncertainty	
C_p	Specific heat	J/kgK
COP_c	Coefficient of operation of the thermoelectric cooler	
COP_{hp}	Coefficient of operation of the heat pump	
I	Current supply to the TEM	A
I_{hp}	Current supply to the heat plate	A
K	Conductance of a TEM	W/K
$\dot{m}_{air}$	Mass flow of the air	Kg/s
$\dot{Q}$	Heat flux emitted to the heat sink	W
$\dot{Q}_c$	Heat flux absorbed by the TEMs	W
$\dot{Q}_h$	Heat flux emitted by the TEMs	W
r	Electric resistivity of a TEM	Ω
R	Thermal resistance	K/W
R_h^{HP}	Thermal resistance of the hot side heat pipe	K/W
R_c^{HP}	Thermal resistance of the cold side heat pipe	K/W
$s_{\bar{R}}$	Random standard uncertainty of the mean	
T_{amb}	Ambient temperature	ºC
T_{air}	Temperature of the air	ºC
T_h	Temperature of the heat source	ºC

T_c^{TEM}	Temperature of the cold side of the TEM	ºC
T_h^{TEM}	Temperature of the hot side of the TEM	ºC
T_{air}^{i}	Temperature of the inlet air	ºC
T_{air}^{o}	Temperature of the outlet air	ºC
U_R	Expanded uncertainty	
v_{air}	Velocity of the air	m/s
V_{hp}	Voltage supply to the heat plate	V
$\dot{W}$	Power supply to the TEMs	W

1. Introduction

The International Energy Agency declared that due to rapidly growing world energy use between 1971 and 2016 the world's total final consumption was multiplied by 2.5 times [1]. The building sector consumes almost the 41 % of the world's energy consumption and constitutes roughly the 30 % of the annual greenhouse gas emissions. Residential energy use was increased in most northern and continental European countries in 2016 in response to meteorological conditions and colder climate, with reported increases between 4 and 8 % [1], meanwhile the energy demand in the building sector is expected to raise by about the 50 % in 2050, and the space cooling demand to triple between 2020 and 2050 [2]. Since buildings definitely account for a significant proportion of the total energy consumption and carbon emissions, it is necessary and urgent to decrease building energy consumption, minimizing the need for energy use through energy-efficient measures and adopting renewable energies [3]. Hence, EU regulators have published the Energy Performance of Building Directive (EPBD) which stablishes that by 2020 all new

building in the EU must be “nearly-zero” energy building (nZEB), which means to reduce the building energy demand and to produce energy on building site (or nearby) [4].

The amount of the energy used in buildings for heating and cooling is approximately the 40 % of the total energy consumption, therefore and alternative energy efficient method is the main motivation of the researchers in this area [5]. Heating and cooling can be obtained by applying a voltage difference to a thermoelectric module (TEM). A thermoelectric cooler-heat pump (TECHP) is a solid-state energy converter that can create a temperature difference when an electric potential is applied to the TEM, thanks to the Peltier effect [6]. The several advantages that these systems present, such as, high reliability, low weight, no moving parts, gas-free, no chemical reaction, environmental friendly, lengthy life spam and easiness on changing from cooling to heating mode, and vice versa [7,8], convert this technology into a promising alternative to achieve comfort into buildings, as it has been already demonstrated [9–12].

In spite of the reduced COP of thermoelectricity, due to the reduced consumption of the nZEBs, approximately 90% less energy for heating and cooling than that demanded by current building standards, the use of TECHPs for HVAC is very promising if special attention is paid to the design of the heat exchangers, which greatly influence the COP and the cooling capacity of thermoelectric systems. The COP values for heating of a thermoelectric heating and cooling unit can vary from 2.5 to 5 just by the modification of the fan speed of its ducts while the COP values for refrigeration vary from 0.4 to 1 [5]; the variation of the overall thermal conductance between 1 and 40 and the rate of thermal conductance from 0 to 2 procure an increase on the COP from 0.12 to 4.2 [11]; the use of gravity assisted heat pipes, instead of air cooled heat sinks, obtained a 64.8 % improvement in the cooling capacity [13]. Moreover, not only the heat exchanger design

needs to be optimized, but also the number of TEMs and consequently their power supply in order to maximize the COP of the systems [9,14,15].

This paper presents a study of a novel TECHP including heat pipes to be located at a nZEB to obtain the comfort temperature both in winter and summer. As the thermal resistance of the heat pipes is drastically defined by their position, if they are on the hot or cold side of the TEMs, a novel thermal characterization methodology is developed. Up to now, the thermal resistances of heat pipes working as designed have been presented, but not having the evaporator at the designed condenser and vice versa, the operation of the heat pipes located on the cold side of the TEMs. This thermal characterization has been used to optimize the operation of a TECHP modifying the current supplied, the number of TEMs, the air volumetric flow and the ambient temperature thanks to the developed and validated computational model. Moreover, the obtained results are impressive for this technology.

2. Methodology for the thermal characterization of the heat pipes

A nZEB has a very high energy performance, with a nearly zero energy demand that has to be covered by energy from renewable sources produced on–site or nearby. Due to the high tightness of their envelope, mechanical ventilation is necessary in order to ensure healthiness. A waste heat recovery unit (WHR) together with a TECHP could be installed at the mechanical ventilation to obtain the comfort temperature at any time of the year. The TECHP provides heating in winter, as Figure 1a) presents, while cooling in summer just by switching the applied voltage to the TEMs. A single TECHP system can operate both, in winter and in summer. In winter the exterior air is heated up subtracting heat from the interior air flow thanks to the applied energy to the system, as Figure 1b) shows, while

the same air flow has to be cooled down in summer, emitting heat to the interior air flow, once more thanks to the energy applied to the system.

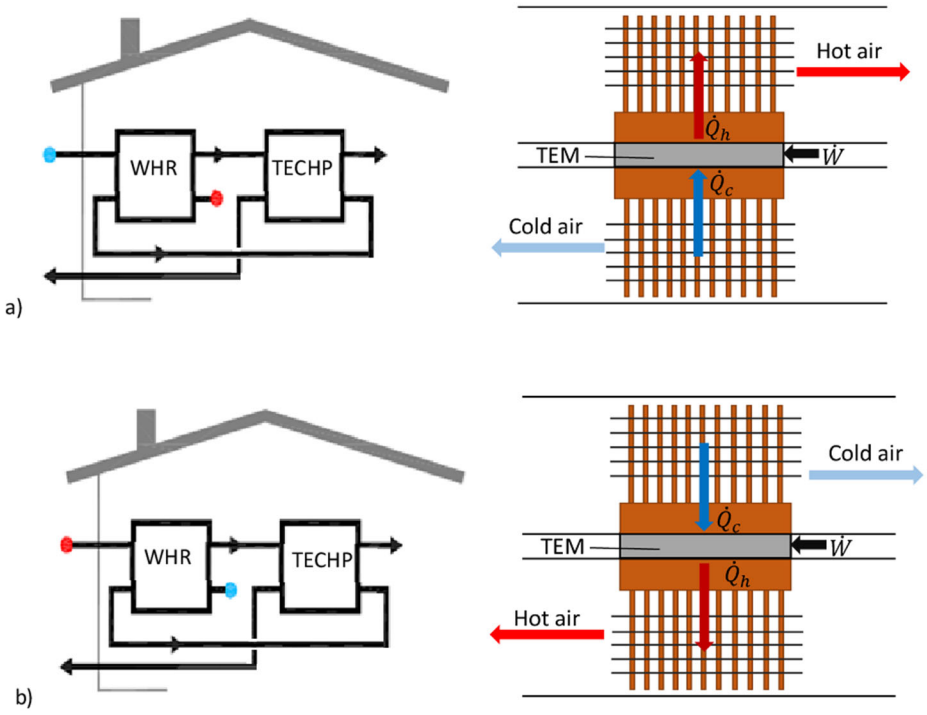

Figure 1. Thermoelectric cooler-heat pump design to be located at a nZEB, a) winter operation, b) summer operation.

A TEM is a solid-state energy converter formed by thermocouples electrically connected in series and thermally in parallel. Each thermocouple is formed by two semiconductors, one n-type and one p-type connected by metallic joints. Two ceramic plates electrically isolate the module and procure rigidity.

Bearing in mind that the heat exchangers play a very important role in the efficiency of thermoelectric systems [16,17], the use of heat pipes has been studied, as they present very good thermal resistances due to their operation principles. The TECHP proposed includes a TEM located between the two air conduits. On each side of the TEM a heat pipe in charge of emitting or absorbing the heat to or from the air flows is included, as it can be observed in Figure 2a). The upper conduit would conduct the external air flow, once it has passed across the WHR system, to the interior of the building; meanwhile, the

lower conduit would conduct the internal air flow that has passed along the WHR system to the exterior. In winter, as Figure 1 a) shows, the heat pipe that is located at the upper conduit, on the hot side of the TEM, works in conventional operation, however, the heat pipe located at the lower conduit, on the cold side of the TEM, works oppositely to its design. During summer, as Figure 1 b) shows, the upper heat pipe, located on the cold side of the TEM, works opposite to its design, while the lower one, located on the hot side of the TEM, works conventionally. Therefore, the heat pipe located on the hot side of the TEM, it does not matter if it is winter or summer, works conventionally while the one on the cold side works opposite to its design. Not only this positioning has been studied, but the same system located horizontally, both conduits laying at the same level, as Figure 2b) presents. This configuration also presents a conventionally working heat pipe and an opposite working one, both in winter and in summer.

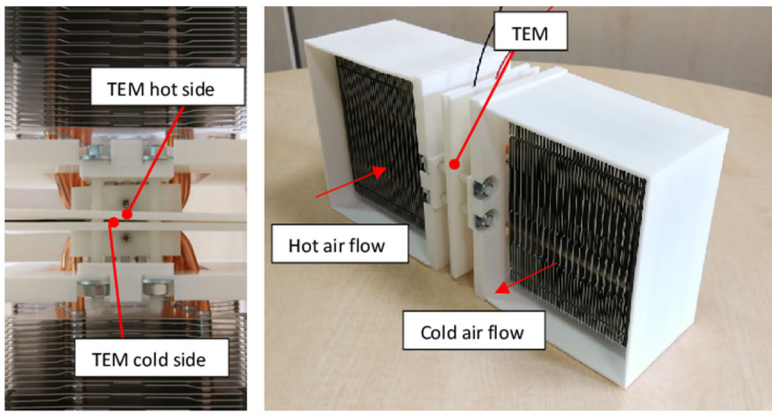

Figure 2. Thermal characterization of the heat pipes, a) detail of the location of the TEM, b) horizontal positon.

The heat pipes used have 5 copper heat pipes of diameter of 6 mm; the evaporator presents a 40 x 40 mm^2 plate to locate the TEM and condensation is helped by fins and forced convection produced by a KD1212PMS1-6A fan at each conduit. The conduits used have a diameter of 12 mm and they have been located both upstream and downstream to make sure that the air flow is ordered.

In order to thermally characterize the heat pipes working as expected and in opposite operation, a methodology has been developed. The thermal resistance of any heat exchanger can be calculated using expression (1), where ΔT stands for the difference in temperature from the heat source to the heat sink and $\dot{Q}$ is the evacuated heat to the heat sink. Thus, the temperature difference from the heat source to the heat sink needs to be known, as well as the heat flux dissipated. The heat flux emitted to the heat source could be calculated using equation (2), but unfortunately, the temperature difference between the inlet and the outlet air at these applications is normally not significant, hence the thermal resistance calculation is inaccurate.

$$R = \frac{\Delta T}{\dot{Q}} \tag{1}$$

$$\dot{Q} = \dot{m}_{air} C_p (T^i_{air} - T^o_{air}) \tag{2}$$

Therefore, the following methodology has been developed in order to accurately thermally characterize the heat pipes. Firstly, the heat pipe working as expected is characterized. To that purpose, the first assembly is done. A single heat pipe is mounted into its conduit, on its evaporator a heat plate is located. The heat plate provides a specific heat flux modifying the electrical input, and the insulation surrounding the system assures that all the heat flux created by the heat plate circulates through the heat pipe ($\dot{Q} = V_{hp} I_{hp}$). The mass flow of the air is determined measuring the velocity of the air at the duct, using an anemometer which precision and accuracy are listed on Table 1, and multiplying by the cross area and the density ($\dot{m}_{air} = v_{air} \rho A$). Figure 3a) shows the prototype, while Figure 3b) the diagram of the mounting used to characterize the heat pipe. Equation (3) includes the expression used to calculate the thermal resistance of the hot side heat pipe (R_h^{HP}).

$$R_h^{HP} = \frac{T_h - T_{air}}{\dot{Q}} \quad (3)$$

a)

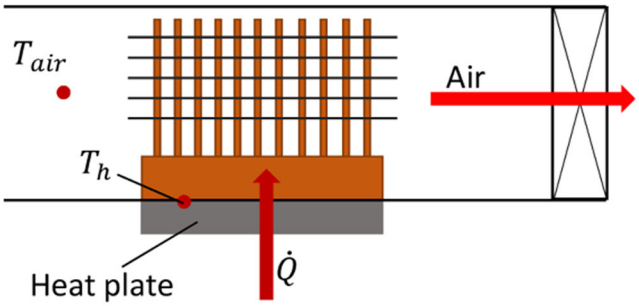

b)

Figure 3. Assembly used to thermally characterize the hot side heat pipe, a) prototype, b) diagram of the assembly.

Table 1. Resolution and accuracy of the measurement probes used.

Sensor	Resolution	Accuracy
Temperature (ºC)	0.1	±0.5
Voltmeter (V)	0.1	±0.2
Ammeter (A)	0.01	±0.02
Anemometer (m/s)	0.01	±0.01 + 3 % measured value

The mass flow of the air ($\dot{m}_{air}$) and the heat flux to dissipate ($\dot{Q}$) determine the thermal resistance of the heat pipe, consequently different levels for both, the mass flow of the air and the heat flux to dissipate have been tested. Figure 4 presents the influence of both parameters on the thermal resistance of the hot side heat pipe for two orientations, horizontal and vertical. An increase of the heat flux to dissipate procures a reduction on the thermal resistance as the phase change heat transfer coefficients, as well as the convective coefficients, improve with an increase of the heat flux. The thermal resistance

decreases from 0.194 to 0.14 K/W, a 38 % reduction, if the heat flux increases from 10 to 50 W. The air mass flow also presents a strong influence on the thermal resistance, as the convective heat transfer coefficient determines the thermal resistance of the heat pipe, and hence improving the convective thermal resistance does have an influence on the overall thermal resistance. Looking at Figure 4 it can be concluded that the thermal resistance of the heat pipe does not change with its orientation, the maximum disagreement between thermal resistances is a 3 %, smaller than the measurement uncertainty, hence no variation of the thermal resistance is obtained if the orientation is changed.

The uncertainty study has been done through equation (4) where b_R stands for the systematic standard uncertainty, $s_{\bar{R}}$ is the random standard uncertainty and the 2 represents a confidence interval of the 95 %. The accuracies of the measurement probes can be consulted at Table 1 and the number of samples is 3 [18].

$$U_R = 2\left(b_R^2 + s_{\bar{R}}^2\right)^{\frac{1}{2}} \tag{4}$$

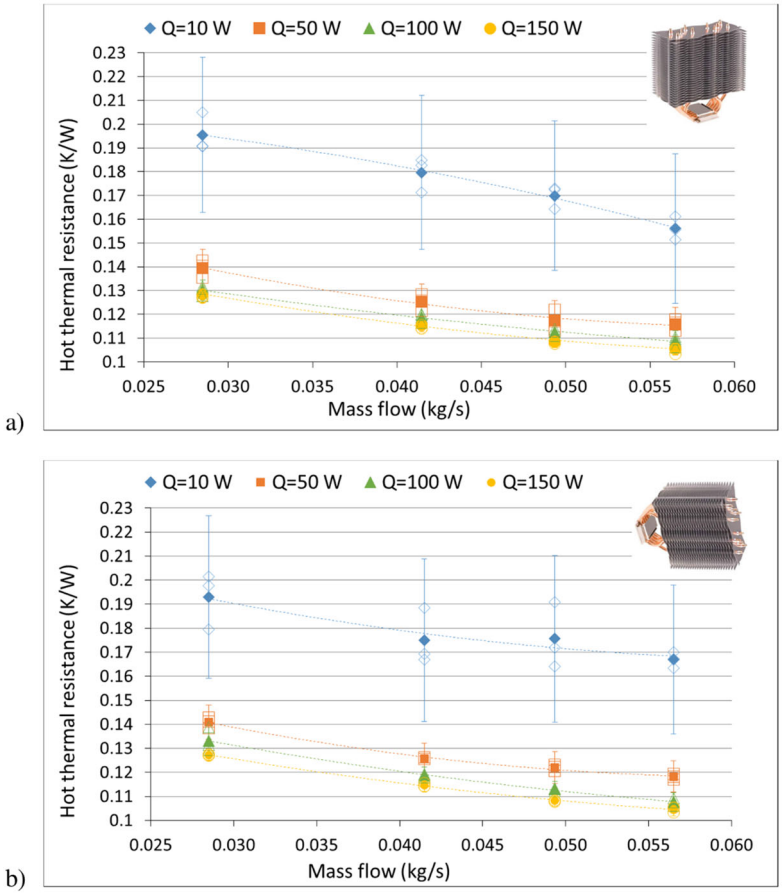

Figure 4. Thermal resistances of the hot side heat pipe, a) vertical position, b) horizontal position.

To thermally characterize the heat pipe of the cold side of the TEM, a novel methodology is proposed. To that purpose an assembly was built, Figure 5 presents this prototype. It is formed by the two conduits, the one that introduces the external air into the building, and the one that emits the interior air of the building to the exterior. A TEM is located between the conduits and the heat pipes on both sides, one on each side respectively. The TEM is connected to a power source which can be manipulated to vary the power. Thanks to the thermal characterization of the heat pipe of the hot side, the heat flux that emits the TEM on the hot side ($\dot{Q}_h$) can be calculated if the temperatures of the hot side of the TEM and the air are known, using equation (5). The thermal resistance of the hot side heat pipe (R_h^{HP}) depends on the heat flux, hence an iterative method is used to obtain the heat flux.

Knowing the heat flux emitted by the hot side of the TEM and the power supplied to the TEM ($\dot{W}$), the power absorbed by the cold side of the TEM ($\dot{Q}_c$) can be calculated using equation (6). Once this heat flux is obtained, the thermal resistance of the heat pipe located on the cold side can be calculated using equation (7).

$$\dot{Q}_h = \frac{T_h^{TEM} - T_h^{air}}{R_h^{HP}} \tag{5}$$

$$\dot{Q}_c = \dot{Q}_h - \dot{W} \tag{6}$$

$$R_c^{HP} = \frac{T_c^{air} - T_c^{TEM}}{\dot{Q}_c} \tag{7}$$

a)

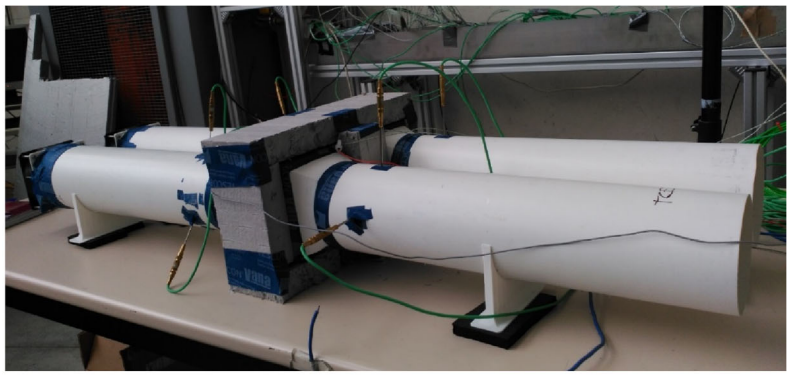

b)

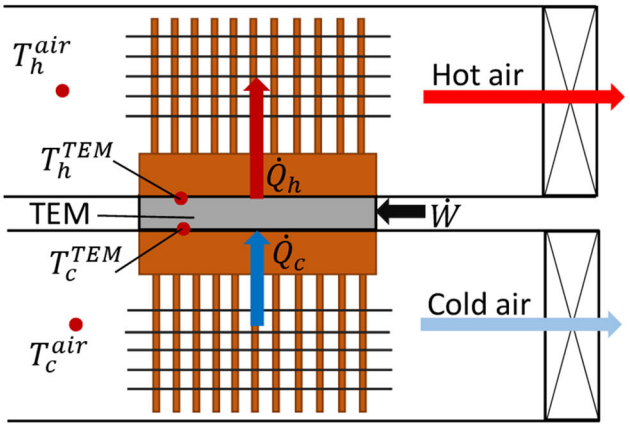

Figure 5. Assembly used to thermally characterize the cold side heat pipe, a) prototype in horizontal position, b) diagram of the assembly.

The thermal resistance of the cold side heat pipe can be observed in Figure 5, presenting two orientations, vertical position (Figure 5a)) and horizontal position (Figure 5b)). The heat fluxes to extract from the air flow are smaller than the ones to dissipate to the other air flow, as presented in Figure 5. The thermal resistances of the cold side heat pipe have duplicated from the ones of the hot side. When the heat pipe is located on the cold side of the TEM it has to work contrary to its design, the evaporator has to be located on the finned end of the tubes while the condenser on the plate, reducing drastically the condensation area and hence increasing its thermal resistance. Due to this operation the thermal resistance worsens drastically as it can be seen in Figure 6. Comparing Figure 6a) and Figure 6b), it can be concluded that the thermal resistances of the heat pipe in vertical position are better than that of the horizontal position. All the areas are similar, thus heat transfer coefficients are the responsible ones for the increase in thermal resistances. Condensation limits the overall thermal resistance, fact that is enhanced as the condensation heat transfer coefficient improves with the vertical position, as condensates leave easier the condensing area letting condensation occur. This fact is also highlighted as the thermal resistance of the cold side heat pipe is not that influenced by the air mass flow as it was the thermal resistance of the hot side heat pipe, as it is not any more the limiting one. Once more, increasing the heat flux decreases the thermal resistance, as it happened when calculating the thermal resistance of the hot side heat pipe.

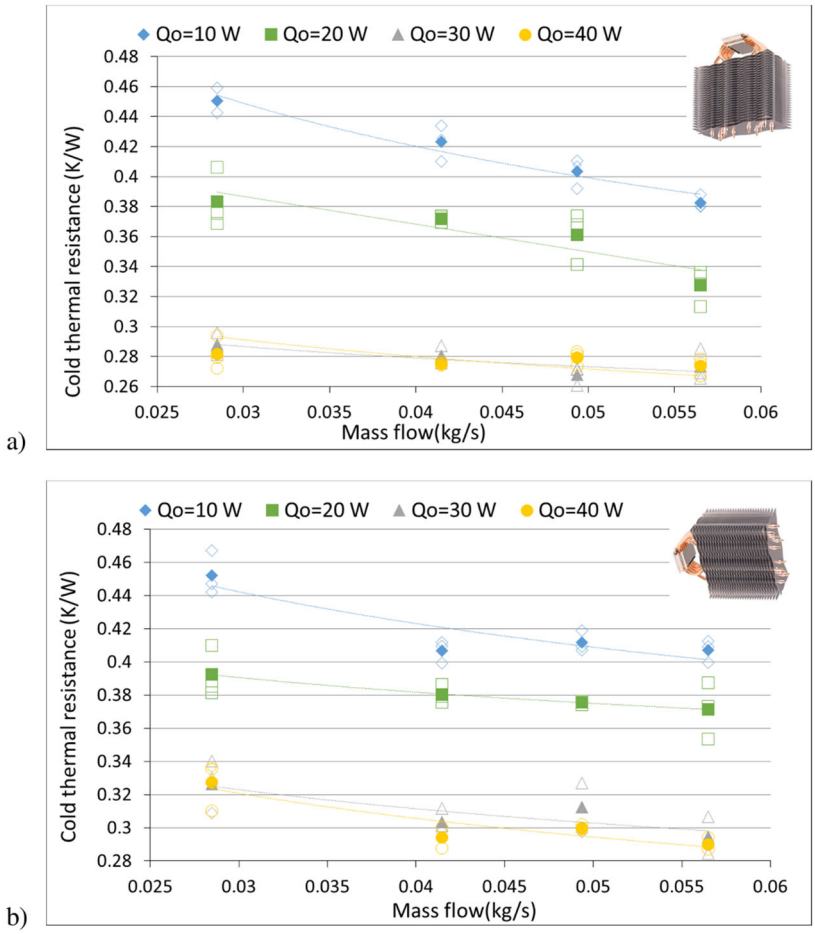

Figure 6. Thermal resistances of the cold side heat pipe, (a) vertical position, (b) horizontal position

The thermal resistance of the heat pipe gets really influenced by its operation. When two heat pipes, one on each side of the TEMs, are located, their thermal resistances are very different as their evaporators and condensers have to be swapped, harming the overall thermal resistance of the heat pipe. Hence, a study of the thermal characterization working on both sides is crucial to optimize the system.

3. Computational modelling

A model that simulates the thermoelectric behavior of the TECHP is proposed. The TECHP should be provided with heat exchangers, on both sides of the TEMs, in order to provide an optimum COP, thus the already studied heat pipes for both sides of the TEM are included into the computational model. The Engineering Equation Solver (EES) software has been used to computationally simulate the thermoelectric and the thermal phenomena. The TEMs simulated are from TE Technology, HP-127-1.4-1.15-71 which present 127 thermocouples with a cross section area of 1.4 x 1.4 mm^2 and a length of 1.15 mm [19]. As the temperatures of the heating or cooling sources are not going to drastically change, the thermoelectric properties are considered constant (at a temperature of 20 ºC), being $\alpha = 0.0541\ V/K$, $K = 0.7166\ W/K$ and $r = 1.3864\ \Omega$ for each BiTe TEM [20].

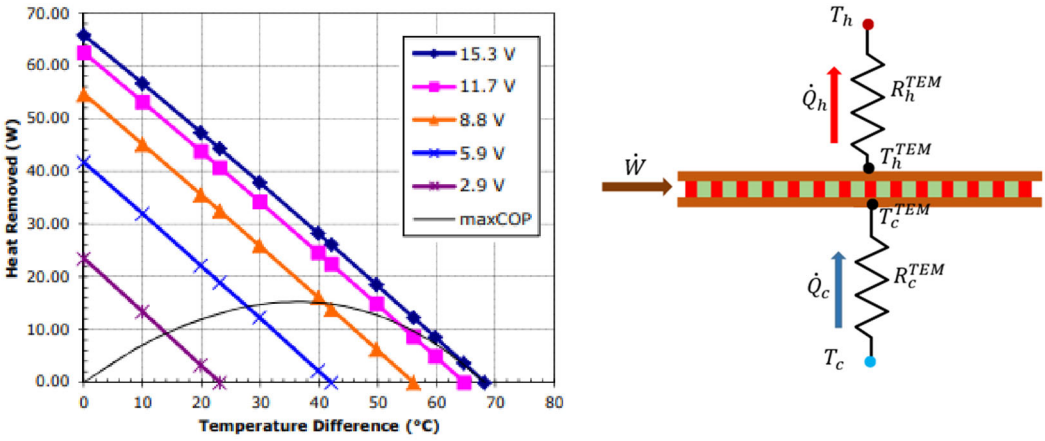

a) b)

Figure 7. TECHP, a) temperature difference of the TEM in function of the applied voltage and heat removed [19], b) schematic of the TECHP.

Figure 7 a) presents the difference in temperature for the TEM as a function of the voltage applied and the heat removed. Figure 7 b) shows the schematic of the TECHP where the heat exchangers on both sides of the TEMs are present as well as the cooling and heating heat fluxes. The energy balance between the cooling or heating source and the heat

exchangers can be defined by equation (8) and equation (9). The cooling and heating heat fluxes are expressed in equation (10) and equation (11), respectively, [21]. The power consumption of each TEM is calculated using equation (12), thanks to an energy balance on the TEM. The previous equations (8)-(12) have to be simultaneously met in order to solve the system, so they are all group together by the computational program and solved, as the five equations present five unknowns (T_h^{TEM}; T_c^{TEm}; $\dot{Q}_h$; $\dot{Q}_c$; $\dot{W}$). The coefficient of performance (COP_c) of the thermoelectric cooler system evaluates the performance of the system, it is the ratio between the cooling heat flux and the consumed power, as can be seen in equation (13).

$$\dot{Q}_c = \frac{T_c - T_c^{TEM}}{R_c^{HP}} \tag{8}$$

$$\dot{Q}_h = \frac{T_h^{TEM} - T_h}{R_h^{HP}} \tag{9}$$

$$\dot{Q}_c = \alpha I T_c^{HP} - \frac{1}{2} I^2 r - K(T_h^{TEM} - T_c^{TEM}) \tag{10}$$

$$\dot{Q}_h = \alpha I T_h^{HP} + \frac{1}{2} I^2 r - K(T_h^{TEM} - T_c^{TEM}) \tag{11}$$

$$\dot{W} = \dot{Q}_h - \dot{Q}_c \tag{12}$$

$$COP_c = \frac{\dot{Q}_c}{\dot{W}} \tag{13}$$

The computational model includes the two air mass flows in counterflow arrangement, the possibility of modifying the number of TEMs used to achieve the comfort temperature within the dwelling, the thermal resistances of the heat pipes obtained in section “2. Methodology for the thermal characterization of the heat pipes”, which are a function of the heat fluxes and the air mass flow, and the possible condensation of the water vapor of the air as the temperature decreases. This model uses the values that the psychrometric

chart of the wet air provides in order to account for the condensation. The enthalpy of the air flow without condensation is compared with the enthalpy at the dew point and if the first one is smaller than the second one the temperature of the air flow is recalculated including the condensation.

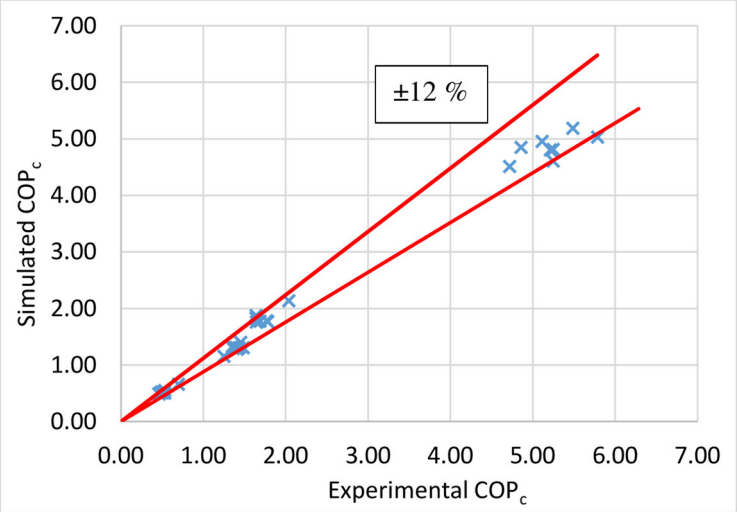

Figure 8. Simulated and experimental values of the COP.

In order to use the computational model to optimize the TECHP, firstly is validated using the obtained data from the thermal characterization of the cold side heat pipe, where the cooling heat flux was calculated to obtain the thermal resistance of the heat pipe. Four cooling heat fluxes (10, 20, 30 and 40 W) and four mass flows of the air where tested for the two configurations, horizontal and vertical position, obtaining a total of 32 experimental cases to validate the computational model. Table 2 and Table 3 include the experimental values of the cooling rate ($\dot{Q}_c$) and its experimental uncertainty, the power supplied to the TEM ($\dot{W}$) and the COP_c for the horizontal and vertical positions, meanwhile they include the computational values for the cooling rate, the consumed power and the COP_c. In order to validate the computational model a contact thermal resistance of 0.1 K/W has been added in between both heat pipes and the thermoelectric module and an electrical efficiency of the 93 %.

Table 2. Experimental and simulated results for the horizontal position used at the validation process of the computational model.

Case	Experimentation			Simulation		
$\dot{m}_{air}$ (kg/s)	$\dot{Q}_c$ (W)	$\dot{W}$ (W)	COP_c	$\dot{Q}_c$ (W)	$\dot{W}$ (W)	COP_c
0.028	10.06 ± 2.19	1.91	5.25	9.00	1.95	4.61
0.041	10.22 ± 2.40	1.73	5.79	8.97	1.78	5.03
0.049	10.31 ± 2.52	1.91	5.25	9.33	1.94	4.82
0.057	10.53 ± 2.81	1.92	5.21	9.47	1.97	4.81
0.028	19.93 ± 3.00	11.22	1.78	20.19	11.39	1.77
0.041	20.44 ± 3.00	11.31	1.77	20.86	11.67	1.79
0.049	19.71 ± 3.23	12.17	1.64	21.69	12.33	1.76
0.057	20.18 ± 3.24	11.84	1.69	21.69	12.19	1.78
0.028	29.99 ± 3.21	24.03	1.25	28.00	24.21	1.16
0.041	30.30 ± 3.67	21.24	1.41	27.48	21.46	1.28
0.049	29.83 ± 3.66	20.22	1.48	26.86	20.56	1.31
0.057	29.82 ± 3.69	20.94	1.43	27.80	21.25	1.31
0.028	39.68 ± 3.53	75.60	0.53	37.47	73.75	0.51
0.041	39.83 ± 3.87	78.62	0.51	39.59	76.09	0.52
0.049	40.31 ± 4.40	79.44	0.50	39.51	77.29	0.51
0.057	40.15 ± 4.46	57.41	0.70	37.69	56.92	0.66

Table 3. Experimental and simulated results for the vertical position used at the validation process of the computational model.

Case	Experimentation			Simulation		
$\dot{m}_{air}$ (kg/s)	$\dot{Q}_c$ (W)	$\dot{W}$ (W)	COP_c	$\dot{Q}_c$ (W)	$\dot{W}$ (W)	COP_c
0.028	10.23 ± 2.23	2.17	4.72	10.01	2.22	4.52
0.041	10.37 ± 2.44	2.14	4.85	9.896	2.04	4.85
0.049	10.57 ± 2.58	2.07	5.11	10.06	2.03	4.96
0.057	10.42 ± 2.78	1.90	5.49	9.88	1.90	5.19
0.028	19.50 ± 2.94	11.88	1.64	21.72	11.85	1.83
0.041	19.87 ± 2.92	12.11	1.64	22.35	12.23	1.83
0.049	19.50 ± 3.20	11.91	1.64	22.53	12.00	1.88
0.057	20.15 ± 3.24	9.89	2.04	21.13	9.89	2.14
0.028	30.60 ± 3.28	22.43	1.36	28.44	21.99	1.29
0.041	30.50 ± 3.69	21.86	1.40	28.69	21.83	1.31
0.049	30.00 ± 3.68	20.67	1.45	28.82	20.52	1.40
0.057	30.31 ± 3.75	22.42	1.35	29.65	22.22	1.33
0.028	40.29 ± 3.59	86.78	0.46	40.24	81.97	0.49
0.041	40.59 ± 3.94	76.63	0.53	40.58	73.83	0.55
0.049	39.57 ± 4.32	86.64	0.46	41.46	83.17	0.50
0.057	39.99 ± 4.45	82.08	0.49	41.45	79.09	0.52

The uncertainty of the cooling power has been calculated using equation (4) and the experimental tests defined in Section 2. The validated model simulates the COP with an error of the ±12 %, as Figure 8 shows.

4. Computational optimization

The validated computational model presented in the previous section simulates the behavior of a TECHP. This model is used to optimize an application where the nZEB standards are used, buildings which require very little energy for their operation, 10 W/m^2 for heating and 7 W/m^2 for cooling [22]. A room of 10 m^2 has been selected, hence in winter 100 W are necessary while in summer 70 W and the inside comfort temperature has been selected to 20 ºC. To that purpose, the current of the TEMs (equation (10) and (11) is modified to meet the application criteria. A WHR system with an efficiency of the 95 % is included, as Figure 1 presents. The influence of the number of TEMs used to achieve the comfort temperature, the influence of the air volumetric flow and the position of the TECHP as well as the influence of the ambient temperature, both in summer and winter is studied using the computational model. TEMs are located one behind the other along 120 mm diameter pipes which bring the exterior air to the enclosure and conduct the interior air to the exterior, respectively.

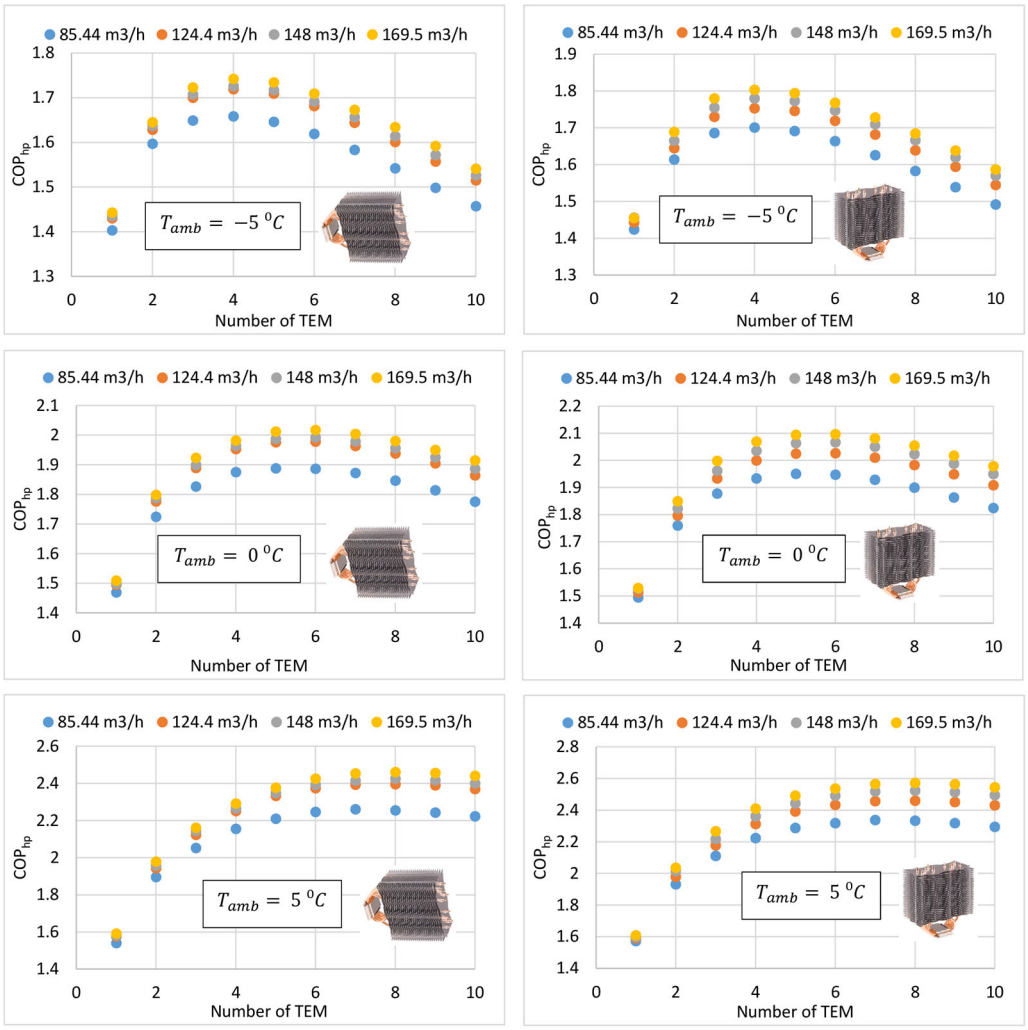

Figure 9. COP_hp for winter operation at different ambient temperatures, for different number of TEMs and air volumetric flows and for the two positions.

To test the performance of the TECHP equation (13) is used for cooling operation (in summer) while equation (14) for heating operation (in winter). As Figure 9 and Figure 10 present, the ambient temperature, the position of the TECHP, the air volumetric flows as well as the number of TEMs determine the operation of the TECHP. As the ambient temperature gets closer to the comfort temperature the COP_{hp} increases and the optimum number of TEMs varies to a greater number. Cool ambient temperatures present optimums COP_{hp} at a smaller number of TEMs, for example if the ambient temperature is $T_{amb} = -5$ °C the optimum number of TEMs is 4 while for an ambient temperature of 5 °C the optimum is at 8. As the number of TEMs increases, each TEM has to supply less

heat to the air flow, hence each one works at a smaller current supply and thus its COP increases [23]. However, the thermal resistances of the heat exchangers located on both sides increase when the heat flux decreases, hence, an optimum for the COP can be found for each ambient temperature. When the ambient temperature is colder, the increase of the thermal resistances due to the reduction of the heat flux is more important than the reduction in the power supplied to each TEM, hence the optimum number of TEMs stays at low values. The vertical position presents higher COPs due to the smaller thermal resistances of the heat pipes located on both sides. This configuration presents advantages for a nZEB as the TECHP is compact enough to be located on the false ceiling and it easies the parallel operation which could be really interesting for these applications.

$$COP_{hp} = \frac{\dot{Q}_h}{\dot{W}} \tag{14}$$

Figure 10 includes the operation of the TECHP in summer at different ambient temperatures, different number of TEMs, different air volumetric flows and for the two positions, horizontal and vertical. Obtaining the comfort temperature with a single TEM is not possible, thus the minimum number of TEMs is two. The same tendencies as the already mentioned for winter operation can be seen. The optimum number of TEMs shifts depending on the ambient temperature, as it is farther from the comfort temperature, the optimum number of TEMs gets smaller. The air volumetric flow has an influence on the coefficients of operation (COP_{hp}, COP_c). In both cases higher air volumetric flows procure higher COPs, as the thermal resistances of the heat pipes decrease if the air volumetric flow increases. For the horizontal position, the air volumetric flow dependency is higher than that for the vertical position, as the thermal resistances of the heat pipes vary to a greater extent if they are collocated horizontally, as Figure 4 and Figure 6 show. The vertical position procures COPs higher than the horizontal position, increases of up to 12 % are achieved in summer while 5 % in winter.

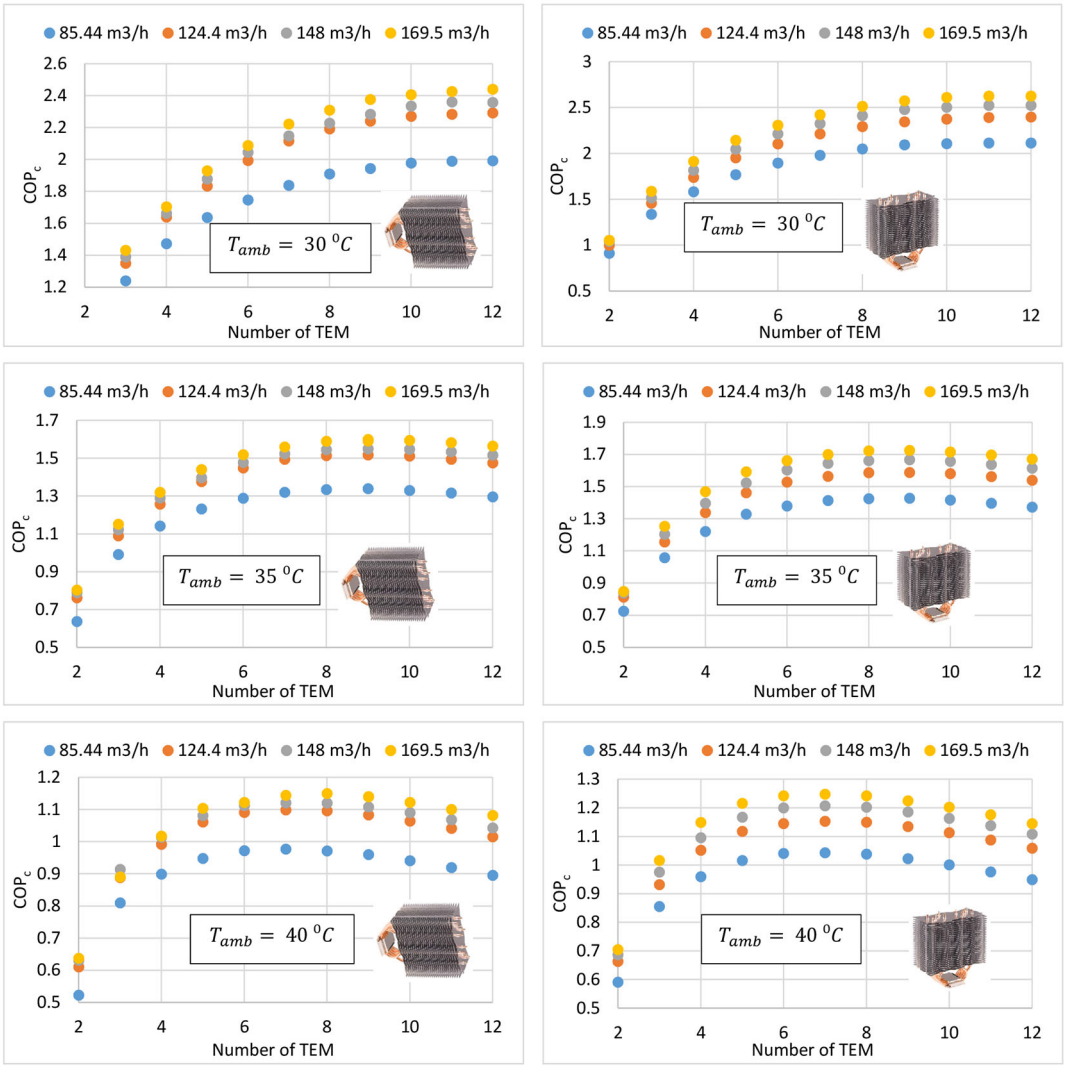

Figure 10. COP_c for summer operation at different ambient temperatures, for different number of TEMs and air volumetric flows and for the two positions.

For summer and winter operation the COPs achieved are very promising, placing this technology as a strong candidate to HVAC of nZEBs. Moreover, the standards of a nZEB are to minimize the energy demand and to provide this little energy demand thanks to renewable energies. Hence, the photovoltaics and TECHPs are a very interesting synergy as both work with direct current, simplifying the electrical installation.

Conclusions

The increased concern about the global warming and the rise in the pollution levels have encouraged new regulations, as the European Energy Performance of Building Directive (EPBD) which dictates public nZEB by end of 2018 and private nZEB by the end of 2020. As the energy demand of this kind of building is small, a TECHP is proposed to HVAC them, both in summer and in winter, as the same device can be used for cooling or heating just switching the power supply. To optimize the operation heat pipes have been proposed, as they present good thermal resistances and they can work both on the cold and hot sides of the TEMs. Their thermal characterization has proven that their operation gets strongly affected if located on the hot or cold side. If their evaporators need to be moved to the designed condenser, and vice versa, their thermal resistances double, hence the developed methodology as well as the thermal resistances obtained are very important to design and optimize the operation of a TECHP run with heat pipes. A validated computational model is used to optimize the TECHP provided with heat pipes on both sides of the TEMs. The number of TEMs, the ambient temperature, the air mass flow and the position are crucial to optimize the operation. The number of TEMs presents and optimum depending on the ambient temperature, as the thermal resistances of the heat pipes increase if the heat fluxes decrease. The optimum number of TEMs decreases if the ambient temperature moves off from the comfort temperature, 20 ºC.

The COPs obtained, both in winter and summer, place the thermoelectricity as a very promising technology to HVAC of nZEBs, as their energy demand is very little. The synergy between thermoelectricity and photovoltaics presents one of the solution to cover the HVAC demand for nZEBs.

Acknowledgments

The authors are indebted to the Spanish Ministry of Economy and Competitiveness for the economic support to this work, included in the DPI2014-53158-R research project.

References

[1] I.E. Agency, World energy balances: Overview, 2018. https://webstore.iea.org/world-energy-balances-2018-overview.

[2] F. Souayfane, F. Fardoun, P.H. Biwole, Phase change materials (PCM) for cooling applications in buildings: A review, Energy Build. 129 (2016) 396–431. doi:10.1016/j.enbuild.2016.04.006.

[3] Z. Liu, L. Zhang, G. Gong, H. Li, G. Tang, Review of solar thermoelectric cooling technologies for use in zero energy buildings, Energy Build. 102 (2015) 207–216. doi:10.1016/j.enbuild.2015.05.029.

[4] O.J.E. Union, EU, Directive 2010/31/EU of the European Parliament and of the Council of 19 May 2010 on the energy performance of buildings, 2010. doi:10.3000/17252555.L_2010.153.eng.

[5] M.Z. Yilmazoglu, Experimental and numerical investigation of a prototype thermoelectric heating and cooling unit, Energy Build. 113 (2016) 51–60. doi:10.1016/j.enbuild.2015.12.046.

[6] K. Irshad, K. Habib, F. Basrawi, N. Thirumalaiswamy, R. Saidur, B.B. Saha, Thermal comfort study of a building equipped with thermoelectric air duct system for tropical climate, Appl. Therm. Eng. 91 (2015) 1141–1155. doi:10.1016/j.applthermaleng.2015.08.077.

[7] A. Rincón-Casado, A. Martinez, M. Araiz, P. Pavón-Domínguez, D. Astrain, An experimental and computational approach to thermoelectric-based conditioned mattresses, Appl. Therm. Eng. 135 (2018) 472–482. doi:10.1016/j.applthermaleng.2018.02.084.

[8] S.B. Riffat, X. Ma, Thermoelectrics: A review of present and potential applications, Appl. Therm. Eng. 23 (2003) 913–935. doi:10.1016/S1359-4311(03)00012-7.

[9] Y.W. Kim, J. Ramousse, G. Fraisse, P. Dalicieux, P. Baranek, Optimal sizing of a thermoelectric heat pump (THP) for heating energy-efficient buildings, Energy Build. 70 (2014) 106–116. doi:10.1016/j.enbuild.2013.11.021.

[10] L. Shen, X. Pu, Y. Sun, J. Chen, A study on thermoelectric technology application in net zero energy buildings, Energy. 113 (2016) 9–24. doi:10.1016/j.energy.2016.07.038.

[11] Y. Cai, S.J. Mei, D. Liu, F.Y. Zhao, H.Q. Wang, Thermoelectric heat recovery units applied in the energy harvest built ventilation: Parametric investigation and performance optimization, Energy Convers. Manag. 171 (2018) 1163–1176. doi:10.1016/j.enconman.2018.06.058.

[12] Z.B. Liu, L. Zhang, G.C. Gong, Y.Q. Luo, F.F. Meng, Experimental study and performance analysis of a solar thermoelectric air conditioner with hot water supply, Energy Build. 86 (2015) 619–625. doi:10.1016/j.enbuild.2014.10.053.

[13] X. Sun, L. Zhang, S. Liao, Performance of a thermoelectric cooling system integrated with a gravity-assisted heat pipe for cooling electronics, Appl. Therm. Eng. 116 (2017) 433–444. doi:10.1016/j.applthermaleng.2016.12.094.

[14] D. Astrain, P. Aranguren, A. Martínez, A. Rodríguez, M.G. Pérez, A comparative study of different heat exchange systems in a thermoelectric refrigerator and their influence on the efficiency, Appl. Therm. Eng. 103 (2016). doi:10.1016/j.applthermaleng.2016.04.132.

[15] A. Attar, H.S. Lee, Designing and testing the optimum design of automotive air-to-air thermoelectric air conditioner (TEAC) system, Energy Convers. Manag. 112 (2016) 328–336. doi:10.1016/j.enconman.2016.01.029.

[16] P. Aranguren, D. Astrain, A. Rodríguez, A. Martínez, Net thermoelectric power generation improvement through heat transfer optimization, Appl. Therm. Eng. 120 (2017) 496–505. doi:10.1016/j.applthermaleng.2017.04.022.
[17] M.F. Remeli, L. Tan, A. Date, B. Singh, A. Akbarzadeh, Simultaneous power generation and heat recovery using a heat pipe assisted thermoelectric generator system, Energy Convers. Manag. 91 (2015) 110–119. doi:10.1016/j.enconman.2014.12.001.
[18] H.W. Coleman, W.G. Steele, Experimentation, Validation, and Uncertainty Analysis for Engineers, 3rd ed, John Wiley & Sons, New Jersey, 2009. http://eu.wiley.com/WileyCDA/WileyTitle/productCd-0470168889.html (accessed February 16, 2016).
[19] TETechnology, HP-127-1.4-1.15-71 dataheet, (2018). https://tetech.com/wp-content/uploads/2013/09/HP-127-1.4-1.15-71.pdf (accessed December 17, 2018).
[20] A. Martínez, D. Astrain, A. Rodríguez, P. Aranguren, Advanced computational model for Peltier effect based refrigerators, Appl. Therm. Eng. 95 (2016) 339–347.
[21] D.M. Rowe, CRC Handbook of Thermoelectrics, New York. 16 (1995) 1251–1256. doi:10.1016/S0960-1481(98)00512-6.
[22] IDAE, Guia del estandar Passivhaus. Edificios de consumo energético casi nulo, 2011. https://www.fenercom.com/pdf/publicaciones/Guia-del-Estandar-Passivhaus-fenercom-2011.pdf.
[23] D. Astrain, A. Martínez, J. Gorraiz, A. Rodríguez, G. Pérez, Computational study on temperature control systems for thermoelectric refrigerators, J. Electron. Mater. 41 (2012) 1081–1090. doi:10.1007/s11664-012-2002-0.